Spherical Modes Driven Directional Modulation With a Compact MIMO Antenna

Abel Zandamela, *Member, IEEE*, Nicola Marchetti, *Senior Member, IEEE*, Max J. Ammann, *Fellow, IEEE*, and Adam Narbudowicz, *Senior Member, IEEE*

***Abstract*—In this letter, a compact beamsteering multiple-input-multiple-output (MIMO) antenna is proposed for directional modulation applications. A generalization of the beamsteering principle is presented and by exploiting the antenna's unidirectional beamsteering capability within the entire azimuth plane, the system realizes secure steerable transmissions in the direction of the legitimate receiver, with a low bit error rate of 10^{-5}, while a high error rate of 10^{-1} is seen outside the desired regions. Numerical and experimental verifications are carried out to validate the proposed concept and comparisons with circular arrays are conducted, revealing that the system achieves comparable performance but with up to 35% and 71% reduction in antenna diameter and profile, respectively. The method is proposed as a good candidate to enhance the security of small Internet of Things (IoT) devices.**

***Index Terms*—Beamsteering antennas, directional modulation (DM), multiple-input-multiple-output (MIMO) antennas, PHY-layer security, small Internet of Things (IoT) devices.**

I. Introduction

PHYSICAL-LAYER (PHY-layer) security methods like directional modulation (DM) are becoming increasingly popular for enhancing secrecy and privacy of wireless communication [1], [2], [3]. As the size and energy constraints of many small Internet of Things (IoT) devices limit the use of sophisticated cryptography, PHY-layer security techniques represent a very promising alternative which exploit the characteristics of wireless channel (e.g., fading and noise) and can be made less computationally expensive. Those features make them a good candidate for improving the security of small IoT platforms.

DM is a keyless PHY-layer security method that relies on beamsteering properties of multiple antennas to transmit an undistorted modulation constellation toward a desired secure direction of the legitimate receiver, while simultaneously spatially distorting the same constellation in other directions, effectively turning it into noise. In state of the art, antenna arrays are used to implement DM schemes [1], [2], [3], [4], [5], [6]. However, antenna arrays require interspacing between elements to reduce the mutual coupling effects. This results in bulky structures that are out-sized for space-constrained IoT devices. Multimodal antennas are a good candidate for multiple-input-multiple-output (MIMO) systems and beamsteering via digital beamforming technology, while also allowing for miniaturization; recent advances in the topic can be found, e.g., in [7], [8], [9], [10], [11], and [12]. To address the size-constraints in IoT scenarios, few works have investigated DM using compact multimodal antennas, e.g., in [13], a dual-mode antenna of $\lambda/2$ diameter is proposed for DM; in [14], a four-mode antenna of 0.7λ diameter is presented for dynamic DM; in [15], a five-mode antenna of 0.65λ is proposed for DM in on-body IoT devices. However, in those works either a relatively large size/profile is still used (limiting their implementation for small IoT scenarios), high side lobes are present (which can be exploited by eavesdroppers to retrieve the transmitted information), experimental verifications are not discussed, or a model highlighting the complete theoretical framework for synthesizing different beam patterns around the azimuth plane, for a given antenna space, is not presented.

In this letter, a compact beamsteering MIMO antenna of 0.55λ diameter is proposed for dynamic DM covering the entire azimuth plane. For the first time, the complete framework of the beamsteering principle is described using spherical modes analysis. Numerical and experimental results demonstrate that a unique secure steerable transmission can be realized with low BER of 10^{-5} at the desired direction, with a high error rate of 10^{-1} outside the legitimate directions. This performance is comparable to a five-element circular array comprising $\lambda/4$ monopoles, while offering 35% miniaturization.

II. Beamsteering Principle and Antenna Configuration

A. Beamsteering Principle

The beamsteering principle can be best explained by using the spherical modes (SMs) analysis, which denotes a set of solutions of the vector wave equation [16]. SMs are commonly used to represent antenna radiation patterns, especially for near-field spherical measurements. The principle is outlined in Fig. 1(b). For this work, the SM will be classified using four indexes (s, l, m, O); where s is related to polarization and for TM waves the magnetic and electric fields are represented by $s = 1$ and $s = 2$, respectively; l ($l = 1, 2, 3 \cdots \infty$) denotes the mode order; m represents the azimuthal phase change and it can take

Manuscript received 4 October 2022; accepted 15 October 2022. Date of publication 19 October 2022; date of current version 3 March 2023. This work was supported by Science Foundation Ireland under Grant 18/SIRG/5612. *(Corresponding author: Abel Zandamela.)*

Abel Zandamela and Nicola Marchetti are with the CONNECT Centre, Trinity College Dublin, The University of Dublin, Dublin 2, Ireland (e-mail: zandamea@tcd.ie; nicola.marchetti@tcd.ie).

Max J. Ammann is with the Antenna and High Frequency Research Centre, School of Electrical and Electronic Engineering, Technological University Dublin, D07ADY7 Dublin, Ireland (e-mail: max.ammann@tudublin.ie).

Adam Narbudowicz is with the CONNECT Centre, Trinity College Dublin, The University of Dublin, Dublin 2, Ireland, and also with the Department of Telecommunications and Teleinformatics, Wroclaw University of Science and Technology, 50-370 Wroclaw, Poland (e-mail: narbudoa@tcd.ie).

Digital Object Identifier 10.1109/LAWP.2022.3215707

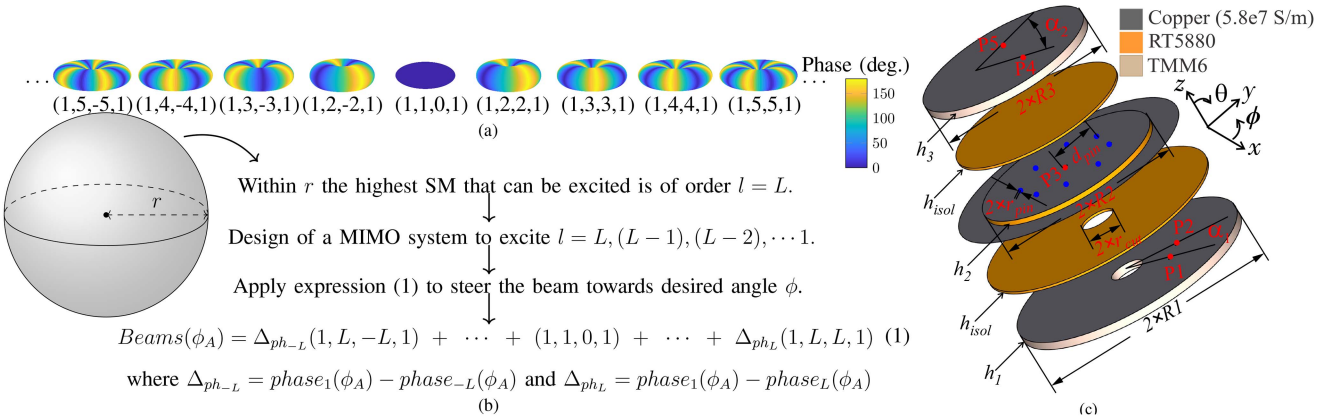

Fig. 1. Proposed beamsteering principle. (a) 3-D phase patterns showing the first few SMs used for this work (for $s = 1$ and $O = 1$). (b) Beamsteering schematic based on the phase control of an MIMO antenna that exploits all the SMs [of type $(1, l, m, 1)$] that can be supported in a sphere of radius r. (c) Exploded-view of the proposed MIMO antenna. Dimensions (in mm): $R_1 = 36.9$, $R_2 = 28$, $R_3 = 26.9$, $r_{\text{cut}} = 5.25$, $r_{\text{pin}} = 0.25$, $h_1 = h_3 = 2.54$, $h_2 = 1.58$, $h_{\text{isol}} = 0.79$, $d_{\text{pin}} = 15$, $\alpha_1 = 225°$, $\alpha_2 = 30°$; feed points P1 = P2 = 16.5, P3 = 0, P4 = P5 = 9.5.

values $-l \leq m \leq l$; finally O characterizes if the mode is omnidirectional ($O = 1$). Please note that O is not an independent variable and is introduced here only to better demonstrate the beamsteering principle. The 3-D phase radiation patterns of the SMs' used for this work are shown in Fig. 1(a). All modes exhibit different phase variations around the azimuth plane and have omnidirectional pattern ($O = 1$) to allow for a 360° coverage. To realize the beamsteering, first we consider that an antenna can be fully enclosed in a sphere of radius r; next the antenna excites an SM of highest order $l = L$, with azimuthal phase variation $m = \pm L$; the principle then investigates an MIMO antenna to excite all SMs of lower order, i.e., $L - 1, L - 2, \cdots 1$. By studying the superposition of SMs', phase control can be introduced to generate constructive interference in given directions along the azimuth plane following (1), where Δ_{ph_l} terms are the phase shifts introduced at the ports exciting phase-varying modes to create the constructive phase interference in the desired angle ϕ_A. The monopole-like (1,1,0,1) mode is used as the reference mode due to its constant phase, and its phase value at a given angle ϕ is denoted by $\text{phase}_1(\phi_A)$. The proposed principle can be realized using digital beamforming technology, with the linear phase variations of the modes allowing to easily predict and synthesize the direction of the beam.

B. Antenna Configuration

Fig. 1(c) shows an MIMO antenna proposed to realize the beamsteering principle discussed in Section II-A. It is comprised of three stacked patch antennas, where each patch is made of copper and designed to operate at the center frequency $f_0 = 2.238\,\text{GHz}$. The bottom and top patches are supported by TMM6 substrate ($\epsilon_r = 6$, $\tan\delta = 0.0023$), with thickness $h_1 = h_3 = 2.54\,\text{mm}$, radius $R_1 = 36.9\,\text{mm}$ (bottom patch), and $R_3 = 26.9\,\text{mm}$ (top patch). Note that a circular hole of radius $r_{cut} = 5.25\,\text{mm}$ is drilled at the center of the bottom patch for the feeding of the middle section. The middle patch is loaded with RT5880 substrate ($\epsilon_r = 2.2$, $\tan\delta = 0.0009$), with $h_2 = 1.58\,\text{mm}$, $R_2 = 28\,\text{mm}$ and is shorted using eight pins of radius $r_{\text{pin}} = 0.25\,\text{mm}$, which are rotated by 45° in respect to the disc center. Note that because the antenna volume is determined by the radius of the highest phase-varying spherical mode (see Fig. 1), materials with lower permittivity can be used for the top and middle layers. For the proposed design, the RT5880 is used in the middle layer as the shorted pins provide size reduction sufficient for (1,1,0,1) mode. Two layers made of RT5880 substrate with thickness $h_{\text{isol}} = 0.79\,\text{mm}$, are used to isolate the middle patch from the bottom and top structures; please note that different substrate materials with other thicknesses are also feasible and may require tuning the antenna parameters. The antenna final dimensions are: $73.8\,\text{mm} \times 73.8\,\text{mm} \times 8.45\,\text{mm}$ or $0.55\lambda \times 0.55\lambda \times 0.063\lambda$.

To generate the (1, 1, 0, 1) mode, the shorting pins are used with the feed point located at the center of the patch [17]. To excite a phase-varying SM_l mode, a feed point can be placed at a radius which provides $50\,\Omega$ impedance match. If the feed point excites $+m/-m$ azimuthal-phase mode, the opposite $-m/+m$ mode of the same order is then obtained by rotating the feed by $\alpha = 90°/l(1 + 2\,k)$, where $k = 0, 1, 2, 3, \cdots$. In the proposed structure the largest patch excites $\text{SM}_{l=3}$, as the highest order; then within the smallest sphere that fully encloses the patch, we can investigate the excitation of five SMs to realize beamsteering: (1, 3, −3, 1); (1, 2, −2, 1); (1,1,0,1); (1,2,2,1); and (1,3,3,1). The $\text{SM}_{l=3}$ are obtained using P1 and P2 oriented by 30° with respect to each other and at a distance of $16.5\,\text{mm}$ from the center, exciting TM_{31} modes. The patterns with $\text{SM}_{l=2}$ are generated from P4 and P5 at $9.5\,\text{mm}$ from the disc center and oriented by 225° with respect to each other, obtaining TM_{21} modes. To enforce the azimuthal phase change, the ports feeding the bottom and top patches are fed with ±90° phase-shift.

The excited modes are shown in Fig. 2(a) and (b). From (1), phase shifts (Δ_{Ph_l}) are introduced in each phase-varying mode, and Fig. 2(c) shows the phase patterns for an exemplar direction, i.e., $\phi_A = 180°$. All the ports are in phase for the desired direction, allowing to synthesize different beam shapes around the azimuth plane, e.g.,: combining $(1, 2, -2, 1)$; (1,1,0,1); and (1,2,2,1) generates a bidirectional beamsteering [shown as blue in Fig. 2(d)]; $(1, 3, -3, 1)$; (1,1,0,1); and (1,3,3,1) produce a pattern with three main beam directions and a combination

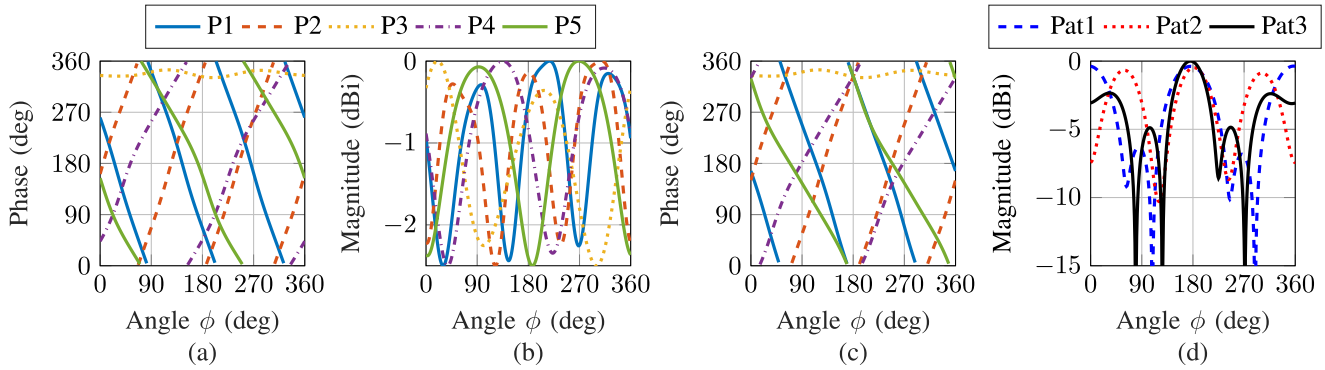

Fig. 2. Synthesized radiation patterns using the proposed MIMO antenna. (a) Phase patterns. (b) Magnitudes of each antenna port. (c) Phase patterns of each port obtained after introducing the phase-shift terms Δ_{ph_l} for $\phi_A = 180°$. (d) Beamsteering performance obtained from expression (1) for $\phi_A = 180°$, where Pat1 represents the combination of $(1, 2, -2, 1)$; (1,1,0,1); and (1,2,2,1) modes; Pat2 is obtained from $(1, 3, -3, 1)$; (1,1,0,1); and (1,3,3,1); and Pat3 is the combination of all the five SMs. Note that only the Pat 3 realizes unidirectional beam pattern within the full azimuth-plane.

of all five modes produces a unidirectional pattern. Note that, the proposed MIMO [Fig. 1(c)] uses the minimum number of modes that can realize unidirectional beamsteering with low side lobes. However, theoretically an infinite number of modes can be excited for better beam control at the cost of size and feeding system complexity. This is explained by the larger diameter needed to support the increased azimuthal-phase change for higher-order SMs (e.g., in the proposed design, the $SM_{l=3}$ modes require $R_1 = 36.9\,\mathrm{mm}$, as compared to $SM_{l=2}$ modes excited using $R_3 = 26.9\,\mathrm{mm}$).

III. Directional Modulation and Experimental Results

This section investigates the antenna beamsteering performance to realize DM technique. For this work, we will assume that the legitimate receiver is located in the azimuth plane at an angle denoted ϕ_{secure}. The dynamic DM transmitted signals for the nth port are given by

$$\text{DMsignal}_n = \frac{\boldsymbol{m}}{SM_n(\phi_{\text{secure}})} \tag{2}$$

where SM_n $(n = 1, \ldots, N)$ denotes the complex patterns of the nth spherical mode in the MIMO system; $\boldsymbol{m} = [(d + s_1), \ldots, (d + s_N)]^T$ is a complex modulation vector; d represents the complex data symbols; without loss of generality, we will assume the use of quadrature phase shift keying (QPSK), resulting in $d \in \{1; j; -1; -j\}$; $\boldsymbol{s}$ is an $N-$element vector used to disperse the constellations. The elements of $\boldsymbol{s}$ are random permutations of the elements of $\boldsymbol{s'}$: a complex vector comprising $\frac{N}{2}$ elements drawn from uniform distribution of $(-1; 1)$ and $(-j; j)$, and its negation $\neg\boldsymbol{s'}$; this gives $\sum_{n=1}^{N} \boldsymbol{s_n} = 0$, ensuring that at the desired ϕ_{secure} direction, the random noise will cancel out. Expression (2) then highlights that the modulated data are transmitted by all the excited SMs with respect to the desired ϕ_{secure} direction. The DM is evaluated by bit error rate (BER) measurements executed in MATLAB using real data obtained from anechoic chamber measurements of the antenna. The measured complex radiation patterns are imported into MATLAB, and a message is then generated and converted to a bitstream for transmission. A total of 10^5 symbols are transmitted with the signal-to-noise ratio at the intended receiver set to $12\,\mathrm{dB}$, and

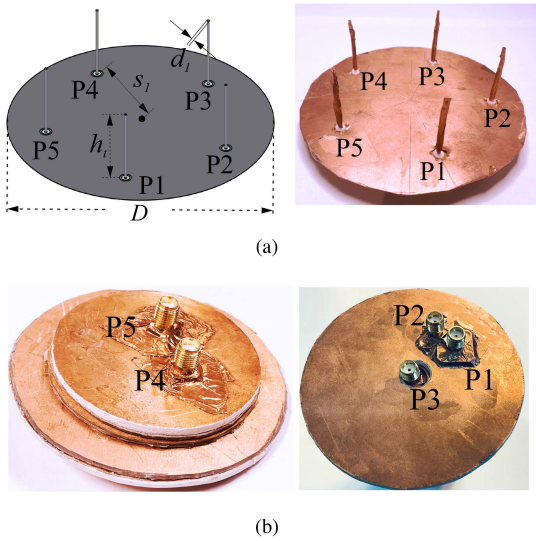

Fig. 3. Investigated antennas. (a) Perspective views of the five-element circular array used for comparisons. (b) Front and back views of the manufactured MIMO antenna. Dimensions (in mm): $d_1 = 1$, $s_1 = 38$, $h_t = 28$, and $D = 106$.

additive white Gaussian noise is assumed to be independent for each location. BER is then obtained by comparing the flipped bits between the demodulated signal and the original one.

First, a five-element circular array is designed for comparison purposes. The array is shown in Fig. 3(a), comprising $\lambda/4$ monopoles and has 0.85λ diameter. The isolation between all the ports at the center frequency is better than $10\,\mathrm{dB}$ and is not shown for brevity. The MIMO antenna and circular array were then manufactured and measured [see Fig. 3(b)], and Fig. 4(a) and (b) shows the simulated and measured S-parameters for the MIMO antenna, respectively. The isolation is better than $17.6\,\mathrm{dB}$ in simulation, and $11.6\,\mathrm{dB}$ in measurements. The $-10\,\mathrm{dB}$ impedance bandwidth overlapping for all ports is $8.5\,\mathrm{MHz}$ in the simulations and $5\,\mathrm{MHz}$ in measurements. Such discrepancies may be explained by manufacturing and assembly tolerances, slight misalignment between the stacked layers and impact of the polyamide hot melt. These deviations were further verified using full-wave simulations.

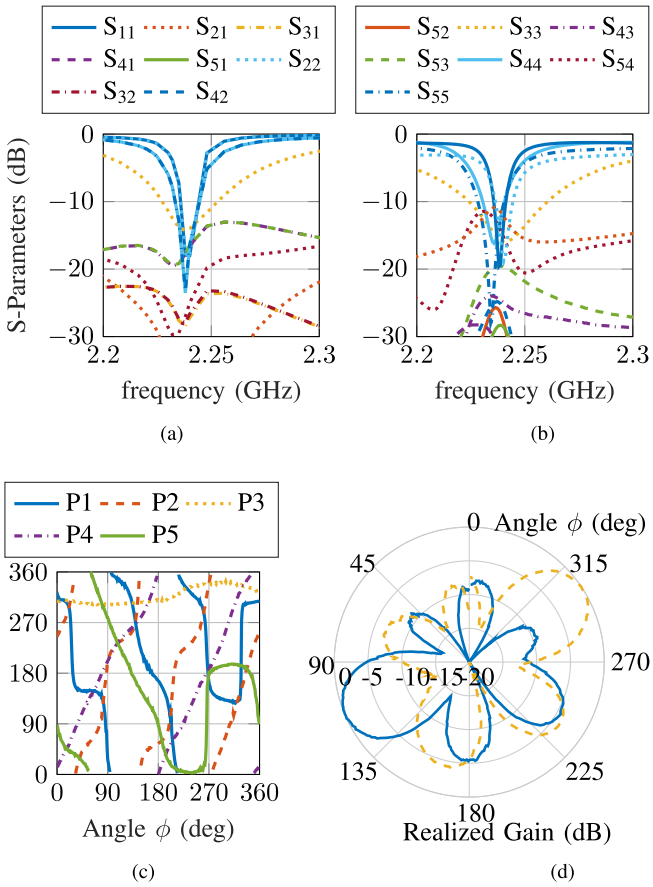

Fig. 4. Measured results. (a) Full-wave simulated S-parameters. (b) Measured S-parameters. (c) Measured phase patterns. (d) Measured normalized realized gain for $\phi = 110°$ (solid lines) and $\phi = 300°$ (dashed lines).

Fig. 4(c) shows the measured phase properties of the proposed antenna. The phase changes linearly for different ports, satisfying the beamsteering conditions from Fig. 1. Some asymmetries are present for P1 and P4 around 270°–310°. This maybe be explained by antenna holder affecting the measurements. Overall, the desired performance is present across the azimuth-plane and the measured beamsteering characteristic is shown in Fig. 4(d) for $\phi = 110°$ and $\phi = 300°$.

Fig. 5(a) and (b) shows the proposed DM for $\phi_{\text{secure}} = 110°$. Fig. 5(a) shows four clear clusters in the IQ plane, representing correct transmissions in the desired secure direction. In contrast, for other eavesdroppers locations [e.g.,: $\phi = 45°$ shown in Fig. 5(b)], the constellations are scrambled making it difficult for illegitimate users to access the transmitted data.

Fig. 5(c) shows BER calculations for the MIMO and circular array in different directions covering the entire azimuth plane. It is seen that the MIMO antenna realizes low BER of 10^{-5} at the desired directions, while outside the desired region a high error rate of 10^{-1} is achieved. The largest beamwidth region with BER $< 10^{-2}$ is $44°$ for the measured MIMO and $61.5°$ for the array structure; this translates into a more secure wireless communication as a much narrower transmission region is realized with the MIMO antenna. It is worth noting that, like most state-of-the-art works [2], [4], [13], [14], the proposed scheme assumes no multipath effect between the transmitter and

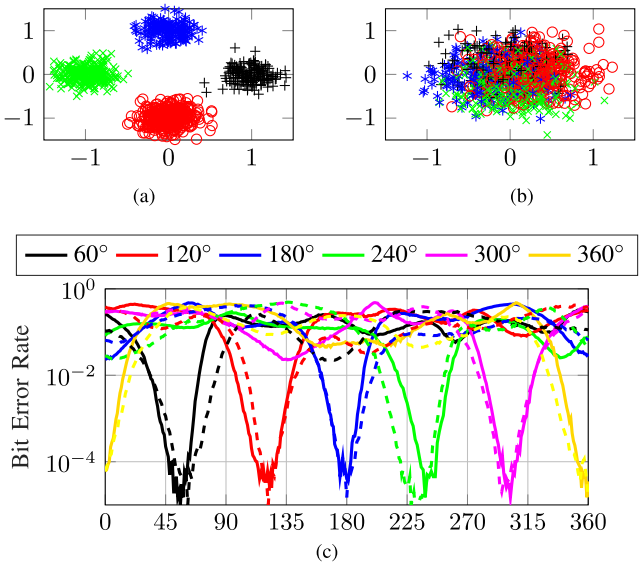

Fig. 5. DM performance. (a) Color-coded QPSK constellations, "00" (black), "01" (red), "11" (green), "10" (blue) for $\phi_{\text{secure}} = 110°$. (b) Eavesdropper at $\phi = 45°$. (c) BER for six different directions separated by 60° covering the xy-plane for measured MIMO (solid lines) and array (dashed lines).

the receiver. Even though DM solutions in multipath channels have been studied in, e.g., [5], [18], [19], in our future work, we will also improve the proposed DM solution in such scenarios, while still addressing the size constraints of small IoT devices. Lastly, while the proposed design shows a narrow bandwidth due to the use of higher order spherical modes, it can support additional security as data transmission is done in a narrower band, which limits the possibility of eavesdropping in different bands. For the connectivity of resource-constrained IoT sensors, such sensors usually require low data-rates, therefore wide bandwidth is usually not required. More importantly, the DM performance is achieved using a structure offering, respectively, 35% and 71% miniaturization in antenna diameter and profile compared to arrays, making our design a good candidate for secure wireless communications in small IoT devices.

IV. Conclusion

This work proposed a compact beamsteering MIMO antenna of 0.55λ diameter. The beamsteering concept was generalized using spherical modes analysis and verified by numerical and experimental studies. The antenna realizes unidirectional beamsteering across the entire azimuth plane, a property exploited to implement directional modulation in small IoT devices. Secure steerable transmissions with largest BER$< 10^{-2}$ beamwidth of $44°$ are realized, while offering substantial size-reductions compared to large array structures (miniaturization up to 35% in diameter and 71% in thickness).

Acknowledgment

The authors would like to thank Jakub Przepiorowski and Neeraj Maurya from Technological University Dublin for their help with antenna measurement and prototyping.

REFERENCES

[1] Y. Liu, H.-H. Chen, and L. Wang, "Physical layer security for next generation wireless networks: Theories, technologies, and challenges," *IEEE Comm. Surveys. Tuts.*, vol. 19, no. 1, pp. 347–376, Jan./Mar. 2017.

[2] Y. Ding and V. Fusco, "Directional-modulation-enabled physical-layer wireless security," in *Trusted Communications with Physical Layer Security for 5G and Beyond*. London, U.K.: Institution Eng. Technol., 2017, pp. 313–336.

[3] X. Ai and L. Gan, "Directional modulation for secure IoT networks via accurate phase response control," *IEEE Internet Things J.*, vol. 9, no. 21, pp. 21537–21547, Nov. 2022, doi: 10.1109/JIOT.2022.3181474.

[4] M. P. Daly, E. L. Daly, and J. T. Bernhard, "Demonstration of directional modulation using a phased array," *IEEE Trans. Antennas Propag.*, vol. 58, no. 5, pp. 1545–1550, May 2010.

[5] Y. Ding and V. Fusco, "A synthesis-free directional modulation transmitter using retrodirective array," *IEEE J. Sel. Topics Signal Proc.*, vol. 11, no. 2, pp. 428–441, Mar. 2017.

[6] C. Sun, S. Yang, Y. Chen, J. Guo, S. Qu, and J. Hu, "4-D retrodirective antenna arrays for secure communication based on improved directional modulation," *IEEE Trans. Antennas Propag.*, vol. 66, no. 11, pp. 5926–5933, Nov. 2018.

[7] F. A. Dicandia, S. Genovesi, and A. Monorchio, "Advantageous exploitation of characteristic modes analysis for the design of 3-D null-scanning antennas," *IEEE Trans. Antennas Propag.*, vol. 65, no. 8, pp. 3924–3934, Aug. 2017.

[8] D. Piao and Y. Wang, "Tripolarized MIMO antenna using a compact single-layer microstrip patch," *IEEE Trans. Antennas Propag.*, vol. 67, no. 3, pp. 1937–1940, Mar. 2019.

[9] Z. Iqbal, T. Mitha, and M. Pour, "A self-nulling single-layer dual-mode microstrip patch antenna for grating lobe reduction," *IEEE Antennas Wireless Propag. Lett.*, vol. 19, no. 9, pp. 1506–1510, Sep. 2020.

[10] K.-L. Wong, M.-F. Jian, and W.-Y. Li, "Low-profile wideband four-corner-fed square patch antenna for 5G MIMO mobile antenna application," *IEEE Antennas Wireless Propag. Lett.*, vol. 20, no. 12, pp. 2554–2558, Dec. 2021.

[11] N. Peitzmeier, T. Hahn, and D. Manteuffel, "Systematic design of multimode antennas for MIMO applications by leveraging symmetry," *IEEE Trans. Antennas Propag.*, vol. 70, no. 1, pp. 145–155, Jan. 2022.

[12] B. Zhang, J. Ren, Y.-X. Sun, Y. Liu, and Y. Yin, "Four-port cylindrical pattern- and polarization-diversity dielectric resonator antenna for MIMO application," *IEEE Trans. Antennas Propag.*, vol. 70, no. 8, pp. 7136–7141, Aug. 2022.

[13] A. Narbudowicz, M. J. Ammann, and D. Heberling, "Directional modulation for compact devices," *IEEE Antennas Wireless Propag. Lett.*, vol. 16, pp. 2094–2097, 2017.

[14] J. Parron, E. A. Cabrera-Hernandez, A. Tennant, and P. de Paco, "Multiport compact stacked patch antenna with 360° beam steering for generating dynamic directional modulation," *IEEE Trans. Antennas Propag.*, vol. 69, no. 2, pp. 1162–1167, Feb. 2021.

[15] A. Zandamela, N. Marchetti, and A. Narbudowicz, "Directional modulation from a wrist-wearable compact antenna," in *Proc. 16th Eur. Conf. Antennas Propag. (EuCAP)*, 2022, pp. 1–5.

[16] J. E. Hansen, ed., *Spherical Near-Field Antenna Measurements (Electromagnetic Waves)*. London, U.K.: Institution Eng. Technol., 1988. [Online]. Available: https://digital-library.theiet.org/content/books/ew/pbew026e

[17] J. Liu, Q. Xue, H. Wong, H. W. Lai, and Y. Long, "Design and analysis of a low-profile and broadband microstrip monopolar patch antenna," *IEEE Trans. Antennas Propag.*, vol. 61, no. 1, pp. 11–18, Jan. 2013.

[18] B. Zhang and W. Liu, "Antenna array based positional modulation with a two-ray multi-path model," in *Proc. IEEE 10th Sensor Array Multichannel Signal Process. Workshop*, 2018, pp. 203–207.

[19] M. Hafez, M. Yusuf, T. Khattab, T. Elfouly, and H. Arslan, "Secure spatial multiple access using directional modulation," *IEEE Trans. Wireless Commun.*, vol. 17, no. 1, pp. 563–573, Jan. 2018.